JOURNAL OF SYNCHROTRON RADIATION
ISSN 1600-5775

First-principles X-ray absorption dose calculation for time-dependent mass and optical density

Viatcheslav Berejnov,[a]* Boris Rubinstein,[b] Lis G. A. Melo[c] and Adam P. Hitchcock[d]

[a]Automotive Fuel Cell Cooperation Corporation, 9000 Glenlyon Parkway, Burnaby, BC, Canada V5J 5J8, [b]Stowers Institute for Medical Research, 1000 East 50th Street, Kansas City, MO 64110, USA, [c]Chemistry and Chemical Biology, McMaster University, 1280 Main Street West, Hamilton, ON, Canada L8S 4M1, and [d]Brockhouse Institute for Materials Research, McMaster University, 1280 Main Street West, Hamilton, ON, Canada L8S 4M1. *Correspondence e-mail: berejnov@gmail.com

Received 16 August 2017
Accepted 13 February 2018

Edited by S. M. Heald, Argonne National Laboratory, USA

Keywords: X-ray absorption; dose integral; STXM; radiation damage.

A dose integral of time-dependent X-ray absorption under conditions of variable photon energy and changing sample mass is derived from first principles starting with the Beer–Lambert (BL) absorption model. For a given photon energy the BL dose integral $D(e, t)$ reduces to the product of an effective time integral $T(t)$ and a dose rate $R(e)$. Two approximations of the time-dependent optical density, *i.e.* exponential $A(t) = c + a\exp(-bt)$ for first-order kinetics and hyperbolic $A(t) = c + a/(b + t)$ for second-order kinetics, were considered for BL dose evaluation. For both models three methods of evaluating the effective time integral are considered: analytical integration, approximation by a function, and calculation of the asymptotic behaviour at large times. Data for poly(methyl methacrylate) and perfluorosulfonic acid polymers measured by scanning transmission soft X-ray microscopy were used to test the BL dose calculation. It was found that a previous method to calculate time-dependent dose underestimates the dose in mass loss situations, depending on the applied exposure time. All these methods here show that the BL dose is proportional to the exposure time $D(e, t) \simeq K(e)t$.

1. Introduction

When a sample is illuminated by X-rays, it takes up the energy of those X-ray photons that are absorbed by the sample. The ratio of the absorbed energy, E, to the mass, M, that absorbs this energy is called the dose: $D = E/M$. If the absorbed energy does not affect the sample in any way and is time independent, then the estimate of the dose is straightforward: one measures the absorbed energy E, the absorbing mass M (hereafter just sample mass) and finds their ratio. In soft X-ray absorption spectromicroscopy (the example used in this paper), the absorbed energy depends on the X-ray photon energy e. In addition, if the chemical properties of the sample change when radiation is applied, then both the absorbed energy E and the sample mass M are time dependent. When the absorbed energy depends on time t and photon energy e, and the sample mass depends on time due to mass loss, the correct dose calculation is less straightforward.

The above problem is common in a series of important applications employing X-rays as a tool for obtaining chemically sensitive structural information for materials. Typical experiments include characterization of complex materials such as polymers (Urquhart *et al.*, 1999), organic semi-

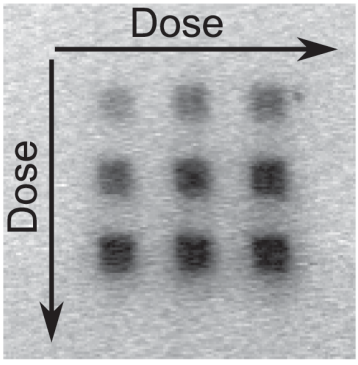

conducting films (Watts *et al.*, 2012; Schuettfort *et al.*, 2012; Collins & Ade, 2012), electrode components of fuel cells (Berejnov *et al.*, 2013) and biological species (Hitchcock *et al.*, 2012) using near-edge X-ray absorption fine-structure spectroscopy (NEXAFS) (Ade & Hitchcock, 2008; Stöhr, 1992), which is the basis for chemical contrast in scanning transmission soft X-ray microscopy (STXM) (Kaznatcheev *et al.*, 2007; Kilcoyne *et al.*, 2003). All the above materials are prone to damage from soft X-ray irradiation. Another type of experiment where dose calculation is important is in quantitative studies of chemical change caused by soft X-ray irradiation (Leontowich, 2013; Tzvetkov *et al.*, 2014; van Schooneveld & DeBeer, 2015; Coffey *et al.*, 2002; Wang, Morin *et al.*, 2009; Beetz & Jacobsen, 2003; Wang, Botton *et al.*, 2009). Such studies help understand radiation damage mechanisms, both from a fundamental perspective (Howells *et al.*, 2009; Leontowich *et al.*, 2011, 2016; Hitchcock *et al.*, 2005) and for practical applications, such as chemical patterning (Wang, Stöver, Hitchcock & Tyliszczak, 2007; Zhang *et al.*, 1995; Leontowich *et al.*, 2012, 2013; Wang *et al.*, 2007; Leontowich & Hitchcock, 2011) and X-ray lithography (Leontowich & Hitchcock, 2011; Leontowich, 2012, 2013). The third type of experiment is protein crystallography where hard X-ray damage is an important obstacle for obtaining the structures of protein crystals (Kmetko *et al.*, 2006; Borek *et al.*, 2010; Paithankar & Garman, 2010; Sliz *et al.*, 2003). In all these experiments, if the radiation dose to the sample is significant, then both the material and the absorbed energy change with time, and the resulted dose is time dependent, affecting the interpretation of the results.

Is there a generalized mathematical framework able to describe the time-dependent dose in such cases? After reviewing the literature (Stolz & Bernhardt, 1981; Pikaev, 1975; Aglincev, 1957; Seltzer *et al.*, 2011; Attix, 1986; Kase & Nelson, 1978) we were not able to find a rigorous general approach for dose calculation when there is significant variation of the absorbed energy and the sample mass with time. This paper develops a general approach and applies it to the case where the irradiation changes of soft X-ray absorption occur with time and are measured by STXM.

STXM measures transmission images of the sample that are converted to optical density images characterizing the local optical density $A(e, t)$, also called OD. The absorbed energy $E(e, t)$ and the mass $M(t)$ are functions of the optical density $A(e, t)$, where all three functions have an instantaneous meaning. Therefore, the correct dose calculation must be formulated in terms of an integral of an instantaneous dose.

Despite the lack of a general approach for time-dependent dose calculations, there have been several attempts (Leontowich *et al.*, 2012; Wang, Morin *et al.*, 2009; Wang, Botton *et al.*, 2009; Wang, Stöver, Hitchcock & Tyliszczak, 2007) using a simplified dose calculation. In these cases the absorbed energy $E(e, t)$ was assumed to be time- and photon-energy-dependent, while the sample mass M was considered to be constant. Hereafter, for simplicity, we will call the dose calculation method reported by Wang, Morin *et al.* (2009), Wang *et al.* (2007) and Wang, Stöver, Hitchcock & Tyliszczak (2007) the 'Wang method', emphasizing the calculus part only. The Wang method uses an effective value $\overline{E}(e, t)$ averaged over the lapsed time interval $(0, t)$ measured at a given e, rather than the instantaneous functions $E(e, t)$ and $M(t)$. Use of this effective $\overline{E}(e, t)$ and constant M reduces the exact dose calculation to the ratio $\overline{D}(e, t) = \overline{E}(e, t)/M$. The Wang method does not involve integration over the variables e and t. Thus, it provides an effective dose $\overline{D}(e, t)$ instead of the actual dose. The relationship between the effective dose $\overline{D}(e, t)$ and the exactly calculated dose $D(e, t)$ is currently unclear.

Here we present an integral formulation for evaluation of the X-ray absorption dose, starting from first principles and applying the Beer–Lambert (BL) model for X-ray absorption (also called the Lambert–Beer law). The discussion is focused mainly on dose calculation with a fixed photon energy (e = constant), over a continuous time interval $(0, t)$. We demonstrate some general properties of the BL dose integral relevant for STXM applications without specifying a particular functional form of the time dependence of the optical density $A(t)$ at a given photon energy e. First, we show that if the photon energy is fixed then the BL dose integral factorizes into a product $D(e, t) = R(e)\,T(t)$, where $T(t)$ is an effective time integral and $R(e)$ is a dose rate (explicitly defined in §3.1). In this case the BL dose integral analysis reduces to an analysis of $T(t)$. Second, we demonstrate that, asymptotically, $T(t)$ is linearly proportional to the elapsed time for sufficiently large time intervals. Third, we present a general analytical approximation for $T(t)$ and estimate the error (residual) relative to an exact formulation. In order to derive the exact $T(t)$ integral expression, a particular functional form of the optical density $A(t)$ must be selected.

Following this, $A(t)$ data for poly(methyl methacrylate) and perfluorosulfonic acid measured by STXM dose-damage experiments are presented and analysed using two approximations: exponential $A(t) = c + a\exp(-bt)$ and hyperbolic $A(t) = c + a/(b + t)$ related to possible first- and second-order kinetics, respectively. For each $A(t)$ approximation we consider the exact expression of the $T(t)$ integral, its approximation and its asymptotics. The exact analytical solutions are based on a combination of exponent integrals $Ei(z) = -\int_{-z}^{\infty}[\exp(-x)]/x\,\mathrm{d}x$ and natural logarithms $\ln(z)$. The derivation was performed using computer algebra software *Mathematica 8.0* (Wolfram Research Inc., IL, USA).

The results of all six calculations of the effective time integral $T(t)$ are compared with those calculated using the Wang method. Depending on how the sample mass is treated, we separately consider the Wang method for constant mass (the original method) and for a time-dependent mass (our extension of the Wang method). The results show that the original Wang method underestimates the dose while all other methods produce curves that are closely aligned to each other. This cluster of $D(e, t)$ curves for the time interval $(0, t)$ can be approximated as $D(e, t) \simeq K(e)\,t$, where $K(e)$ is a function of the photon energy and some other parameters, but independent of time. This finding allows $A(t)$ to be converted into $A(D)$ by stretching the time axis by the factor K for both optical density models considered.

2. First-principles dose calculation

Assume that a sample, homogeneous in all three dimensions, is exposed to soft X-ray photons all with energy e and absorbs a dose $D(e, t)$ at time t. What is the increment of dose δD over a time increment δt? Following the dose definition introduced above, we find an expression for the change of absorbed energy $\delta E(t)$ that the sample of time-dependent mass $M(t)$ received in the time interval $(t, t + \delta t)$. Their ratio is the dose change $\delta D(t)$ which should be integrated to obtain a formula for the dose absorbed over any lapsed time $(0, t)$. The increment of the absorbed energy is an integral over the time increment $\delta E(t) = \int_t^{t+\delta t} \dot{E}(x)\,\mathrm{d}x$, where $\dot{E}(t)$ is an absorbed energy rate (the number of absorbed photons of energy e per unit of time) and x is an integration variable. The photon energy e is fixed and omitted for clarity. Assuming the time increment δt is infinitely small, the above integral can be computed in linear approximation $\delta E(t) = \dot{E}(t)\,\delta t$. The sample mass is a function of time only (we will clarify this statement below) and it changes from $M(t)$ to $M(t + \delta t)$. We introduce a sample mass $m(t)$ for this time interval and approximate the mass by the average $[M(t) + M(t + \delta t)]/2$. Expanding $M(t + \delta t)$ in Taylor series and retaining only the first-order term, we find $m(t) = M(t)(1 + \alpha)$, where $\alpha = [M'(t)/2M(t)]\,\delta t \ll 1$. Here, and in subsequent equations, $' = \mathrm{d}/\mathrm{d}t$ denotes the derivative with respect to t. Collecting all parts together and retaining the lowest order in δt, the expression for the dose increment is

$$\delta D(e, t) = \dot{E}(e, t)\,\delta t/M(t). \tag{1}$$

The dose at any moment t can be found by computing the following integral,

$$D(e, t) = \int_0^t \frac{\dot{E}(e, x)}{M(x)}\,\mathrm{d}x. \tag{2}$$

The above formula states that, for the dose calculated at moment t, the time evolution of both the energy absorption rate and the sample mass must be *already known* at least to the moment t. From a practical point of view we can measure the functions $\dot{E}(e, t)$ and $M(t)$ by standard sampling. Note that equation (2) is the special case of a fixed photon energy corresponding to irradiation by a monochromatic X-ray beam and continuous time exposure spanning the interval $(0, t)$.

3. Dose formulation for the BL model of X-ray absorption

3.1. BL dose integral

In STXM (Ade & Hitchcock, 2008; Kilcoyne *et al.*, 2003) a beam of soft X-ray photons of energy e hits the sample with a rate i_0 (number of photons per second). Because the STXM beam is monochromated, under exposure the photon energy e is fixed, while time is a continuous variable. Thus, in the general expression for energy- and time-dependent optical density $A(e, t)$, the photon energy can be omitted keeping only the time-dependent part $A(t)$, a function of a single variable t. The detector, which is positioned right behind the sample along the beam axis, collects a transmitted rate i of photons of the same energy. Since the detector is not ideal, it measures k times less photons than hit the sample, and thus the true photon rates are i_0/k and i/k, respectively, where k is a photon-energy-dependent detector efficiency coefficient $[0 < k(e) < 1]$. We also assume that the sample is homogeneous within the size of the X-ray beam (typically 30–50 nm). The real STXM makes an image by raster scanning the sample (or, less commonly, the zone plate imaging optics) with a pixel size of 10–100 nm. If the sample changes its chemical properties, then the rate of transmitted photons becomes time dependent, $i(t)$. A rapid in-vacuum beam shutter is used such that the sample is only exposed during the actual measurement from 0 to t. The incident, i_0, and transmitted, $i(t)$, detector photon rates are related through the BL absorption model (BL model, for short), $i(t) = i_0 \exp[-A(t)]$, where $A(t)$ is the optical density, and all functions are given for the fixed photon energy e. The BL model is a solution of a differential equation describing the attenuation of the X-ray intensity i by an infinitesimal layer of material $\mathrm{d}h$: $\mathrm{d}i = -i(h)\mu\,\mathrm{d}h$, where, in the framework of the BL model, the decay of intensity $\mathrm{d}i$ is proportional to i and μ is a constant coefficient related to the particular absorption of the sample material. Thus, for the case of a sample thickness which is dependent on time $h(t)$, we have $A(t) = h(t)\mu$.

The rate of energy absorption $\dot{E}(e, t)$ from the absorbed photons is $i_0 - i(t)$ multiplied by the photon energy e. The mass $M(t)$ of the material in the beam cross section is a product of the cross-sectional area of the beam s, the material density ρ and the sample thickness $h(t)$: $M(t) = h(t)\rho s$, where mass is a function of time only. The thickness of the sample can be expressed in terms of the optical density $A(t)$ and μ, where μ is the standard absorption coefficient (or linear absorption coefficient), which is a function of the photon energy $\mu(e)$. The method of obtaining $\mu(e)$, having a dimension of inverse length [when the dimension used is 1 nm, μ is also known as an OD1 coefficient (Hitchcock *et al.*, 2012)], is presented elsewhere (Ade & Hitchcock, 2008). Substituting the expressions for the rate of absorbed energy and change in sample mass into the dose equation (2) we arrive at the BL dose integral for an exposure time t (the upper limit of the integral), where constants and all parameters depending only on the photon energy e are extracted from the time-dependent integrand (Appendix *A*),

$$D(e, t) = \frac{e i_0 \mu(e)}{k(e)\rho s} \int_0^t \frac{1 - \exp[-A(x)]}{A(x)}\,\mathrm{d}x. \tag{3}$$

Knowledge of the evolution of optical density $A(t)$ with exposure time is essential for computing the BL dose integral equation (3) and is usually obtained from STXM experiments. A dimensional analysis shows that the constant $R(e) = [e i_0 \mu(e)]/[k(e)\rho s]$ is a *dose rate*, which is a function of the photon energy. $R(e)$ is the dose absorbed in 1 s by a 1 nm-thick layer of a pure material at its standard gravimetric density whose optical density is equal to the standard absorption coefficient (OD1) at photon energy e.

The ratio $D(e, t)/R(e)$ is an integral $T(t)$ that has the dimension of time. We call it an *effective time integral*,

$$T(t) = \int_0^t \frac{1 - \exp[-A(x)]}{A(x)}\, \mathrm{d}x. \tag{4}$$

Here the numerator $1 - \exp[-A(x)]$ is the fraction of the incident photons that are absorbed in a moment x (x is a time integration variable, not a coordinate) and the denominator is the optical density $A(x)$ of the thickness of the material absorbing these photons. We denote the dimensionless integrand $\{1 - \exp[-A(x)]\}/A(x)$ in equation (4) as the function $F[A(x)]$. Then the dose reads

$$D(e, t) = R(e)\, T(t), \tag{5}$$

$$T(t) = \int_0^t F[A(x)]\, \mathrm{d}x, \quad F(x) = [1 - \exp(-x)]/x. \tag{6}$$

Therefore, in this case the calculation of the BL dose integral is reduced to a calculation of the effective time integral $T(t)$ from equation (4) or equation (6). The constant $R(e)$ is calculated for the conditions of the STXM experiment and is time independent.

Equation (3) estimates the dose collected per pixel when STXM is imaging at a fixed photon energy. This formula can be applied for mapping the dose as well as for calculating the average dose for an image or for a series of images used in spectromicroscopy. Image series are also called stacks (Jacobsen *et al.*, 2000). Below we use this expression to evaluate dose in 9-pad dose studies (Leontowich, 2012; Wang, 2008).

3.2. BL dose integral asymptotics for large time

Experiments carried out for different elapsed times (Coffey *et al.*, 2002; Beetz & Jacobsen, 2003; Leontowich *et al.*, 2012; Wang, Botton *et al.*, 2009) show that $A(t)$ evolves from an initial value A_0 to a constant value A_∞ at large time exposure, as shown in Fig. 1. We want to find a functional form of $D(e, t)$ for large exposure time, which is the asymptote of the BL dose integral as $t \to \infty$. We split the interval of the $A(t)$ argument into two segments: $0 < t < t^*$ where $A(t)$ changes significantly, and $t > t^*$ where $A(t) \simeq A_\infty$. The behaviour of the dose at large times can be written as (Appendix *B*)

$$D(e, t) \simeq R(e)\, [E(t^*) + Bt], \tag{7}$$

where $E(t^*) = C(t^*) - Bt^*$ is a composite constant dependent on t^* determined by a particular optical density evolution $A(t)$, and $R(e)$ is a term independent of time. From a practical perspective the time t^* sets a scaling of the dose $D(e, t^*)$, and can be related to the so-called critical dose defined as the dose for $A(t)$ to decay from A_0 to $A(t^*)$. Here we introduce two constants,

$$B = \frac{1 - \exp(-A_\infty)}{A_\infty}, \tag{8}$$

and

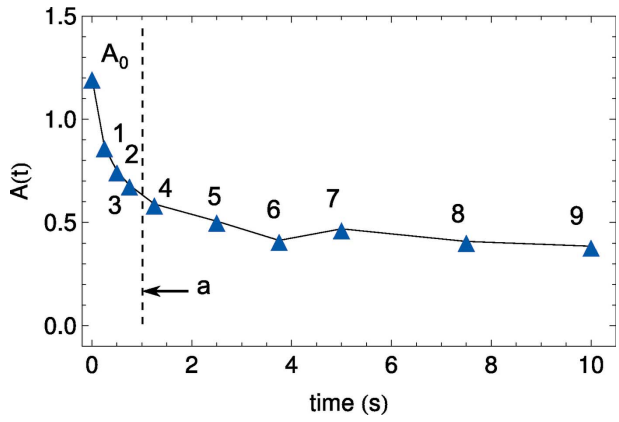

Figure 1
Decay of optical density $A(t)$ with elapsed time for the STXM dose-damage data presented in Fig. 2. Each point is the optical density averaged over the inner constant OD area, of each pad. The value at $t = 0$ is measured from an area not previously exposed. The solid curve is a linear approximation between every two points. The dashed line (a) denotes the $A(t)$ variation over 1 s of exposure (blue triangles in Fig. 3).

$$C(t^*) = \int_0^{t^*} \frac{1 - \exp[-A(x)]}{A(x)}\, \mathrm{d}x. \tag{9}$$

For the specific case when the value $A_\infty \ll 1$ is small but still positive we obtain $B \simeq 1$. The constant $R(e)$ is a combination of experimental parameters (e, i_0 and s) dependent on the beam properties while ρ, μ and A_∞ are related to the properties of the material. The coefficient μ is specific to the particular material in its initial chemical state assuming that this material is chemically stable upon X-ray exposure (Henke *et al.*, 1993; Ade & Hitchcock, 2008). The coefficient A_∞ represents the limiting value of the optical density $A(t)$ at long time exposure in cases where the sample stops changing with exposure (it may reach 0 in some cases).

3.3. Analytical approximation for the BL dose integral

An exact integration of the BL dose integral is possible for some selected optical density functional dependencies $A(t)$, but in general this task can be performed only numerically. Here we derive an approximate general method, the BL dose integral analytic expression. We require that this approximation has an appropriately small difference from the exact result (*i.e.* a small residual) for a practically significant time interval.

Equation (5) reduces the problem of calculation of the BL dose integral equation (3) to calculation of the effective time integral $T(t)$ given by equation (4). First, a function $a(t)$ [which is the running average of the optical density $A(t)$] is introduced *via* the relation

$$A(t) = a(t) + a'(t)t = [ta(t)]' \quad \text{or} \quad a(t) = (1/t) \int_0^t A(x)\, \mathrm{d}x. \tag{10}$$

Then the approximation for $T(t)$ becomes

$$T(t) = \int_0^t F[A(x)]\,\mathrm{d}x \simeq tF[a(t)] = \frac{1-\exp[-a(t)]}{a(t)}\,t, \qquad (11)$$

providing an estimate of the effective time integral with a residual error $O(t)$ which is considered in Appendix *C*. The result reads

$$O(t) = T(t^*) - T_a(t^*) = \int_0^{t^*} \frac{1-\exp[-A(x)]}{A(x)}\,\mathrm{d}x - \frac{1-\exp[-a(t^*)]}{a(t^*)}\,t^*. \qquad (12)$$

Note that an expression for $a(t)$ similar to equation (10) was used by Wang *et al.* (Wang, Morin *et al.*, 2009) [formula (4) therein] as an exponential approximation of the optical density $A(t)$. The residual of our approximation $tF[a(t)]$ is defined for the interval $0 < t < t^*$. The last equation shows that $O(t)$ is a constant and its value depends on t^* and on a particular functional dependence of the optical density $A(t)$, which can be found from an approximation of STXM data like those presented in Fig. 1.

4. Approximate models of optical density for STXM applications

4.1. STXM dose – damage study

One type of dose dependent study with STXM involves the generation of a pattern with controlled variation of the soft X-ray exposure (Leontowich *et al.*, 2012; Wang, Botton *et al.*, 2009; Wang, Morin *et al.*, 2009). An example of this, one involving a 3 × 3 (9-pad) pattern generated in a perfluorosulfonic acid (PFSA) thin film, is presented in Fig. 2(*a*). The exposure time for each pad is incremented in order to obtain nine well defined doses, which are intentionally varied in a non-linear time pattern reflecting non-linearity of $A(t)$. After generating the 9-pad pattern, the whole region of 9-pads is imaged at one or more photon energies with an exposure time short compared with the pattern generation doses, in order to visualize the non-damaged and damaged parts of the material and quantify $A(t)$. The 9-pad transmission images are converted to optical density images $A(x, y, e) = \ln[i_0(e)/i(x, y, e)]$, where the functions $A(x, y, e)$ and $i(x, y, e)$ are values at each (x,y) pixel, while $i_0(e)$ is the same for all pixels and measured off the sample, but including the underlying substrate if that exists under the sample material.

The radiation damage displayed in Fig. 2(*a*) is significant and leads to a clear decay of optical density (darker areas). At the photon energy used, the optical density of the pads progressively decreases as the exposure time increases. (NB: there are photon energies in the C 1*s* edge at which the OD of damaged PFSA increases with dose.) The set of nine optical density values constitutes the experimental measurement of $A(t)$ (Fig. 1). Fig. 2(*b*) shows the typical spectra measured for non-damaged and damaged samples of the PFSA membrane, and their ratio.

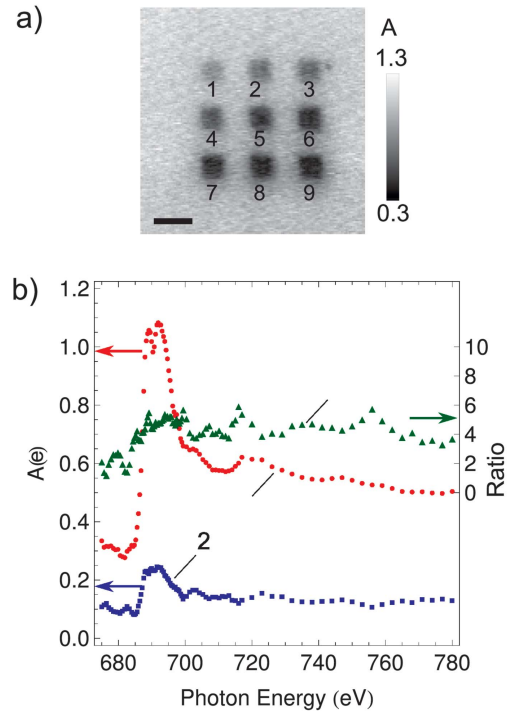

Figure 2
(*a*) Optical density image of an STXM 9-pad pattern for damage of a ∼100 nm-thick microtomed section of PFSA. The transmission signal was measured at 694 eV (second peak in the F 1*s* spectrum) with 1 ms dwell time. The *i* signal, measured for areas on the PFSA sample but outside the 9-pads, is 1.8 (1) × 10^4 counts, and the i_0 intensity, measured off the PFSA section, is 5.7 (2) × 10^4 counts. The grey scale is the optical density (absorbance, *A*). The scale bar is 1 µm. (*b*) F 1*s* absorbance [optical density, $A(e)$] spectrum of a PFSA sample [different than the one patterned in (*a*)], measured with STXM under no damage (red, 1) and large exposure (blue, 2) conditions. The ratio of the undamaged to damaged spectra is plotted (green, 3) (right-hand intensity scale).

4.2. Approximations of the experimental optical density from STXM data

An expression for the evolution of optical density with exposure time $A(t)$ is required for dose calculation. The STXM 9-pad experiment, Fig. 2(*a*), provides $A(t)$ data for a given photon energy (Fig. 1). What function is suitable for approximating the $A(t)$ data in Fig. 1? From a dose calculation perspective $A(t)$ is just a tool for its calculation and any kind of functionality is allowed as long as it follows the data with reasonably small mean square error.

However, Fig. 1 demonstrates that $A(t)$ is a function of the dose itself, as for longer exposure we have a larger dose and lower optical density. $A(t)$ is linked directly to the changed chemical bonding of the radiation damaged material; the evolution of optical density in $A(t)$ reflects chemical processes taking place in the irradiated material. Thus, from this perspective, the function $A(t)$ cannot be selected arbitrarily but should have some specific form related to the kinetics of the radiation damage processes. Currently, there is a widespread assumption (Wang, Morin *et al.*, 2009; Wang, Botton *et al.*, 2009; Beetz & Jacobsen, 2003; Wang, Stöver, Hitchcock & Tyliszczak, 2007; Zhang *et al.*, 1995; Leontowich *et al.*, 2012)

that the $A(t)$ decay (Fig. 1, Fig. 3) is an exponential function $A(t) = c + a\exp(-bt)$ (model 1) related to radiation-induced chemical reactions and/or physical processes which follow first-order kinetics (Zhang *et al.*, 1995). In addition to model 1, we introduce here a hyperbolic decay of optical density $A(t) = c + a/(b + t)$ (model 2) corresponding to second-order kinetics. STXM data analysis and dose evaluation are performed for both models in order to demonstrate the flexibility of our method for a variety of dose-damage experiments, including those where the order of kinetics is different from one.

The analysis of STXM data we present here is common in physics. We test whether the proposed heuristic functionality produces unbiased residuals. The method involves transforming the coordinates such that multiple datasets collapse to a single straight line, making the residuals visually evident. This approach still does not indicate whether the chosen functionality is the best for all data, but it significantly narrows down the types of approximation functions which may represent the correct scaling underlying the available data sets.

To illustrate both cases of optical density evolution we consider five STXM 9-pad data sets, three of which were obtained for PFSA membrane, *i.e.* PFSA (Nafion™), and two for poly(methylmethacrylate), *i.e.* PMMA thin films. These materials have significantly different spectroscopic changes upon soft X-ray irradiation. In addition, different film fabrication processes, film thickness, patterning photon energy and damage imaging photon energy were used for each set. The raw $A(t)$ data for these data sets are presented in Fig. 3.

First we introduce two approximate functions, $y = c + a\exp(-bx)$ (model 1) and $y = c + a/(b + x)$ (model 2), where x denotes the time coordinate. Then we transform the x, y coordinates into new X, Y coordinates in order to collapse the original data: $Y = (y - c)/a$, $X = xb$, giving $Y = \exp(-X)$ for model 1; and $Y = (y - c)/a$, $X = b + x$, giving $Y = 1/X$ for model 2. These coordinate transformations allow us to convert the data presented in Fig. 3, where the $A(t)$ law is obscured due to data complexity, and plot them in coordinates where the $A(t)$ functionality becomes apparent. The practical approach is the following: each set of data is a least-squares fit to a particular model and the coefficients a, b and c are found. Then, for given $y = A(t)$ and $x = t$, the new coordinate values X and Y are calculated. The results are presented in Fig. 4.

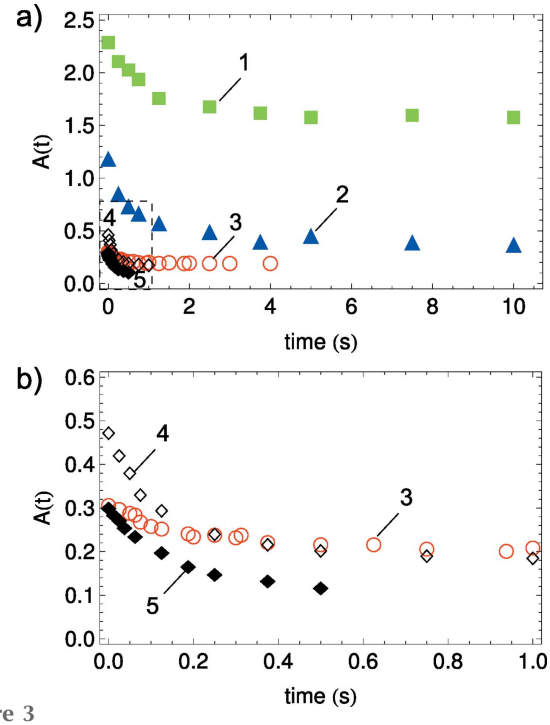

Figure 3
(*a*) Optical density $A(t)$, measured using STXM 9-pad dose experiments, plotted with respect to the exposure time. Microtome film of NRE211 membrane (PFSA): green squares (1), C 1*s* patterning and imaging at 292.6 eV; blue triangles (2), F 1*s* patterning and imaging at 694 eV. Spin-coated DuPont-D521 ionomer (PFSA): red circles (3), patterning and imaging at 320 eV. Spin-coated PMMA film #1: black open diamonds (4), patterning at 300 eV, imaging at 288.45 eV. (Sample prepared and data measured by A. F. G. Leontowich.) Spin-coated PMMA film #2: black filled diamonds (5), C 1*s*, patterning at 320 eV imaging at 288.45 eV. All imaging is performed with 1 ms dwell, all patterning exposure times are incremented non-linearly. (*b*) Expansion of the dashed box in (*a*).

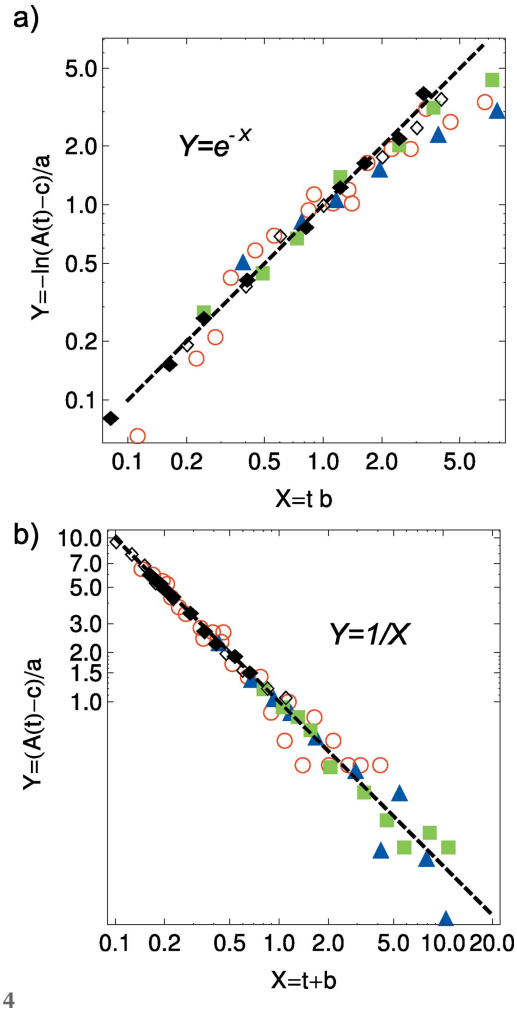

Figure 4
STXM 9-pad dose data in Fig. 3 plotted using rescaled X and Y coordinates for (*a*) model 1 (exponential) and (*b*) model 2 (hyperbolic). Both plots are presented using bi-natural logarithm scaling. Note that the Y coordinate for model 1 is transformed by applying $-\ln(Y)$ to make a linear function.

Table 1
Relative mean square error (ξ^2) along the $y = A(t)$ axis for each of the approximation cases.

Each column corresponds to the number of the data sets presented in Fig. 3.

STXM data	#1 $\times 10^{-3}$	#2 $\times 10^{-3}$	#3 $\times 10^{-3}$	#4 $\times 10^{-3}$	#5 $\times 10^{-3}$
Model 1, ξ_1^2	0.8	3.1	2.7	0.13	0.65
Model 2, ξ_2^2	1.1	0.6	1.4	0.16	0.31
$\xi_1^2 - \xi_2^2$	−0.3	2.5	1.3	−0.03	0.34

The dashed lines in Figs. 4(*a*) and 4(*b*) represent the heuristic $A(t)$ dependence we are testing against the real STXM data. Note that both dashed curves have a 45° inclination, since all plots are in bi-natural logarithmic scaling. Table 1 presents the relative mean square error along the $y = A(t)$ axis for both models, where the absolute mean square error is scaled by the difference $\mathrm{Max}[A(t)] - \mathrm{Min}[A(t)]$ for each data set presented in Fig. 3.

The relative error for both models is 1–3%, which is considered very good from an experimental perspective. The exponential model 1 (first-order kinetics) produces a larger relative error (residual) for most of the data sets except #1. In addition, the residuals of model 1 have a clear *bias* in Fig. 4(*a*) along the fit, while the residuals of model 2 are *distributed* evenly along the fit, Fig. 4(*b*). We also studied a bi-exponential model and found that it does not remove the above bias for residuals. The analysis of Table 1 suggests that model 2 (second-order kinetics) seems to have a better agreement with STXM data than model 1, but the difference is not sufficient to reliably determine the order of the kinetic reaction. This quite important and rather unexpected conclusion is discussed in §7.

5. Calculating the BL dose integral for both $A(t)$ models

The selection of a particular $A(t)$ model defines the effective time integral $T(t)$. The general solution of the $T(t)$ integral for a given time interval $(0, t)$ can be explicitly found either by exact integration or by using the approximate function given in equation (11). If the general solution of $T(t)$ is known, then the BL dose integral $D(e, t)$ is the product of the $R(e)$ constant and $T(t)$ according to equation (5). Each particular model $A(t) = c + a\exp(-bt)$ or $A(t) = c + a/(b + t)$ must be fit against STXM data to generate the values of empirical constants a, b and c that allow evaluation of the general expression, equation (5), and thus obtain the dose $D(e, t)$ for a given photon energy e and exposure time t. In this part we present the $T(t)$ integral, its exact analytical solutions, and functional approximations regarding both models of the exposure-dependent change in optical density.

For analytical integration the argument of the integrand function $F[A(t)]$ is replaced by $F(y)$ where y is a new integration variable. If we introduce a new function $y = A(x)$, then the integration variable is expressed as $x = g(y)$ and its differential is $\mathrm{d}x = g'(y)\,\mathrm{d}y$. Substituting these expressions into the $T(t)$ integral gives

$$T(t) = \int_0^t \frac{1 - \exp[-A(x)]}{A(x)}\,\mathrm{d}x \;\rightarrow\; T(y_1, y_2) = \int_{y_1}^{y_2} \frac{1 - \exp(-y)}{y}\,g'(y)\,\mathrm{d}y, \tag{13}$$

where $T(y_1, y_2)$ is a new definition of the effective time integral, $y_1 = A(x = 0)$ and $y_2 = A(x = t)$ are new integration limits. The function $g'(y)$ depends on the optical density model $A(t)$. For calculation of $T(t)$ *via* its approximation by equation (11), the function $a(t)$ must be found explicitly using equation (10).

5.1. Model 1: $A(t) = c + a\exp(-bt)$

5.1.1. Exact integration for $T(t)$. For model 1 we have $y = c + a\exp(-bt)$, $t = g_1(y) = \ln[a/(y - c)](1/b)$, $g_1'(y) = -1/[b(y - c)]$ and the effective time integral after substitution reads

$$T(y_1, y_2) = -\int_{y_1}^{y_2} \frac{1 - \exp(-y)}{y}\,\frac{1}{b(y - c)}\,\mathrm{d}y = T_1(y_2) - T_1(y_1). \tag{14}$$

The indefinite integral $T_1(y)$ is quite cumbersome (Appendix *D*1). For compactness we introduce a new function $\Phi_{\pm}(q, p)$, where $\Phi_{\pm}(q, p) = \exp(-p)\,Ei(p - q) - \ln[\pm(p - q)]$. The expression for $T_1(y)$ then reads

$$T_1(y) = \frac{\Phi_{-}(y, c) - \Phi_{-}(y, 0)}{bc}, \tag{15}$$

and the exact solution of the effective time integral for model 1 is

$$T(t) = T_1[c + a\exp(-bt)] - T_1(c + a). \tag{16}$$

To calculate the effective time integral and then the dose, a time interval $(0,t)$ has to be set and $A(t)$ obtained. The experimental data are fit to produce the a, b and c coefficients, which allow calculation of $y_1 = c + a$ and $y_2 = c + a\exp(-bt)$. Then evaluation of all Φ_{-} components for given a, b, c, y_1 and y_2 produces $T(t)$ (Appendix *D*1). Finally, by computing $R(e)$ for the given photon energy, we calculate the dose $D(e, t)$.

5.1.2. Approximation of $T(t)$. Substituting the optical density $A(t)$ for model 1 into equation (10) and integrating we have an expression for a product $a(t)\,t = ct - a[1 - \exp(-bt)]/b$. Note that $a(t)$ and a are the approximation function and the fitting parameter of $A(t)$, respectively, and should not be mixed up. Dividing the above expression by t does not make $a(t)$ divergent at small times. Indeed, by applying L'Hospital's rule we can find a limit of $a(t)$ for small t: $a(0) = c + a$. Therefore, the final formula for $a(t)$ reads

$$a(t) = c - a\,[1 - \exp(-bt)]/(tb). \tag{17}$$

To calculate the approximated value of the BL dose integral, equation (17) must be substituted into equation (11) to find

$T(t)$. Then $T(t)$ is substituted into equation (5) and, for the given $R(e)$, the dose $D(e, t)$ can be computed.

5.2. Model 2: $A(t) = c + a/(b + t)$

5.2.1. Exact integration for $T(t)$. The substitution functions for model 2 are $y = c + a/(b + t)$, $t = g_2(y) = a/(y - c) - b$ and $g_2'(y) = -a/(c - y)^2$. The effective time integral for this case after substitution is

$$T(y_1, y_2) = -\int_{y_1}^{y_2} \frac{1 - \exp(-y)}{y} \frac{a}{(c - y)^2}\, dy = T_2(y_2) - T_2(y_1), \quad (18)$$

where

$$T_2(y) = -\frac{a[1 - \exp(-y)]}{c(c - y)} - \frac{a}{c^2}\Big[c \exp(-c)\, Ei(c - y) + \Phi_+(y, c) - \Phi_+(y, 0)\Big]. \quad (19)$$

The exact solution of the effective time integral for model 2 reads

$$T(t) = T_2[c + a/(b + t)] - T_2(c + a/b). \quad (20)$$

The calculation of the dose for model 2 is similar to that for model 1. The only difference is that the STXM data must be fit with the hyperbolic model 2, which produces different values of a, b and c. The expanded version of equation (20) is given in Appendix *D*2.

5.2.2. Approximation of $T(t)$. The expression $a(t)$ for model 2 is similar to that for model 1. The integration of equation (10) gives $a(t)\, t = ct + a \ln(b + t) - a \ln(b)$. The limit of $a(t)$ for small t for model 2 is $a(0) = a/b + c$, and the final formula for $a(t)$ for model 2 is

$$a(t) = c + (a/t) \ln(1 + t/b). \quad (21)$$

To calculate the approximate value of the BL dose integral, equation (21) must be substituted into equation (11) and the result substituted into equation (5), which, for a given $R(e)$, gives the dose value $D(e, t)$.

6. BL dose evaluation for different $A(t)$ models and integral calculation methods

This section compares dose computation $D(e, t)$ by several methods: the exact integral solution, the functional approximation, the asymptotic expression, the Wang method (Wang, Morin *et al.*, 2009; Wang *et al.*, 2007; Wang, Stöver, Hitchcock & Tyliszczak, 2007; Wang, Botton *et al.*, 2009; Zhang *et al.*, 1995; Beetz & Jacobsen, 2003; Leontowich *et al.*, 2012) and an extension of the Wang method that we introduce. Because $R(e)$ is the same for all of these methods, the dose computation is reduced to an evaluation of the effective time integral $T(t)$, equation (4). For calculating $T(t)$ the optical density approximation $A(t)$ should be chosen and fitting coefficients a, b and c obtained by fitting the experimental data. Since we consider two models of the $A(t)$ approximation, *i.e.* exponential and hyperbolic, we have two sets of approximation coefficients. This gives ten different dose computations in total for the given $A(t)$ data set. Among all the data sets presented in Figs. 3 and 4 we select the one measured for PFSA: blue triangles (2), the patterning and imaging for which were performed at 694.0 eV, the second peak in the F 1*s* spectrum (Susac *et al.*, 2011). This data set is well suited for demonstration because it has a long time interval and a large decay of $A(t)$. The conclusions of this section can be applied to all data sets in Figs. 3 and 4. Table 2 presents the approximation coefficients obtained by least-squares fitting these data with models 1 and 2. The time variable for all of these $T(t)$ calculations is always given in seconds.

Table 2
Approximation coefficients for least-square fitting both models against the PFSA data obtained by STXM dose experiments at 694 eV (second peak in the F 1*s* spectrum).

		a	b	c
Model 1	$A(t) = c + a\exp(-bt)$	0.725	1.553	0.437
Model 2	$A(t) = c + a/(b + t)$	0.354	0.429	0.368

6.1. Comparison of exact integration *versus* functional approximation

Figs. 5 and 6 present the exact and approximate $T(t)$ solutions for model 1 and model 2, respectively. The exact solution is the black solid curve calculated from equation (16) for Fig. 5(*a*) and from equation (20) for Fig. 6(*a*). The functional approximation solution is a red dashed curve calculated by substitution into equation (11) of equation (17) for Fig. 5(*a*), and of equation (21) for Fig. 6(*a*). The residue $\Delta T(t)$ (the difference between the exact solution and the approximate one) is presented in Figs. 5(*b*) and 6(*b*) for both models, respectively. The relative difference $\delta T(t)$ (the residue divided by the exact solution) is presented in Figs. 5(*c*) and 6(*c*). The residuals presented in Figs. 5(*b*) and 6(*b*) increase with time more slowly than the nearly linear increase of $T(t)$ presented in Figs. 5(*a*) and 6(*a*). Because of this, the relative difference in Figs. 5(*c*) and 6(*c*) reaches a maximum of $\sim$0.9% (0.7%) and then decays with respect to the exposure time for model 1 and 2, respectively. The low value of the relative difference <1% for both $A(t)$ models indicates that equation (11) is a good general form of the functional approximation.

6.2. Exact integration: comparison of model 1 and model 2

The STXM data presented in Fig. 3 can be collapsed into single curves (Fig. 4) when the scaling of $A(t)$ is chosen properly. Model 2 (hyperbolic) provides a somewhat better representation than model 1 (exponential). How does this difference affect the $T(t)$ exact integral solution? The answer is presented in Fig. 7. Both models, a solid black curve for model 1 and a red dashed curve for model 2, produce $T(t)$ functions that match quite well for the entire time interval (0,10) s. Fig. 7(*b*) represents the comparison over a more extended time interval, (0,100) s. It plots the difference of the exact $T(t)$ solution for model 2 minus that for model 1. Within

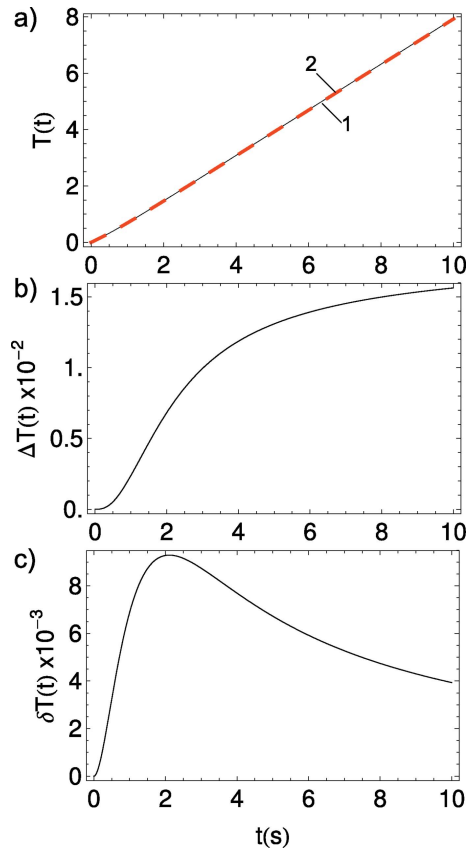

Figure 5
Optical density $A(t)$ for model 1 (exponential). (*a*) $T(t)$ integral calculations; the black solid curve (1) is the exact calculation by equation (16), and the red dashed curve (2) shows the approximation of equation (11). (*b*) Residue $\Delta T(t)$. (*c*) Relative error $\Delta T(t)/T(t)$.

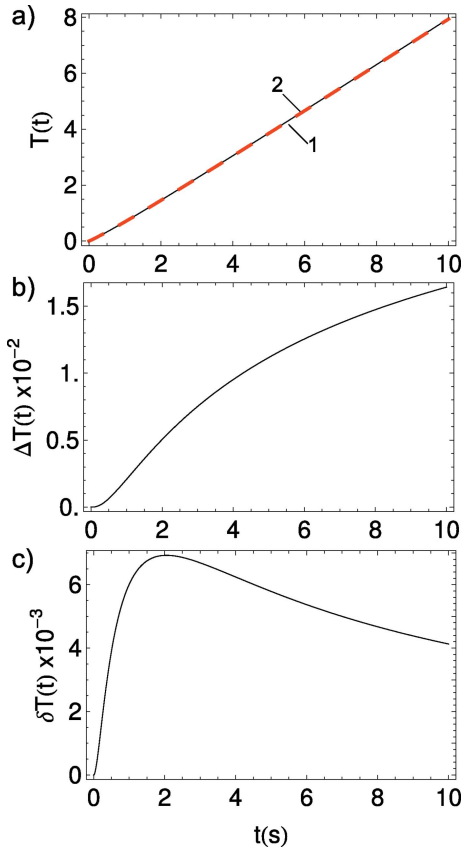

Figure 6
Optical density $A(t)$ for model 2 (hyperbolic). (*a*) $T(t)$ integral calculations; the black solid curve (1) is the exact calculation by equation (20), and the red dashed curve (2) shows the approximation by equation (11). (*b*) Residue $\Delta T(t)$. (*c*) Relative error $\Delta T(t)/T(t)$.

the time interval (0,10) s there is a relative difference of ∼4%. Thus, the choice of the $A(t)$ approximation model affects the exact dose calculation by less than 4% for the actual exposure times used.

6.3. Functional approximation: comparison of model 1 and model 2

Calculation of the $T(t)$ integral by the functional approximation method for both models gives very similar plots with respect to those presented in Fig. 7 (exact integration); the difference is not distinguishable by eye. Thus, to highlight the small deviation in Fig. 7, Fig. 8 plots $\Delta T(t)$ (Fig. 8*a*) and $\delta T(t)$ (Fig. 8*b*) for the functional approximation solutions (red curves) with respect to the exact $T(t)$ integral solutions (black curves). Fig. 8 supports our conclusion that the chosen functional approximation [equations (10) and (11)] is remarkably good for estimating $T(t)$ and thus the BL dose integral.

6.4. Asymptotic dose calculation for model 1 and model 2

The full form of the asymptotic BL dose is given by equation (7). Assuming that the BL dose $D(t)$ for the experimental time intervals can be reduced to the last term of equation (7), then

$$D(t) \simeq R(e)\, B(A_\infty)\, t, \tag{22}$$

where, according to equation (8), the constant $B(A_\infty)$ depends on A_∞ determined by the function approximating $A(t)$ for the particular STXM data with respect to the selected model. Equation (22) is very simple: all coefficients are easy to evaluate, and thus it can be used as a coarse estimate of the BL dose integral. Fig. 9 illustrates how close the dose estimated by equation (22) is to the exact analytical dose calculated for the two approximate models of $A(t)$. As usual, instead of equation (22), we consider the part of the effective time integral $T(t) \simeq B(A_\infty)\, t$. Fig. 9(*c*) demonstrates that the quality of the dose estimated by its asymptotics provides reasonable values [$\delta T(t) < 10\%$] for exposure times of more than 2 s for model 1 and of more than 4 s for model 2.

6.5. $T(t)$ integral calculation: comparison with the Wang method

The Wang dose calculation (Wang, Morin *et al.*, 2009; Wang *et al.*, 2007; Wang, Stöver, Hitchcock & Tyliszczak, 2007; Wang, Botton *et al.*, 2009; Leontowich *et al.*, 2012) reduces the dose calculation to a simple ratio $\overline{D}(t) = \overline{E}(t)/M$, where $\overline{D}(t)$, $\overline{E}(t)$ and M are the effective dose, absorbed energy and the

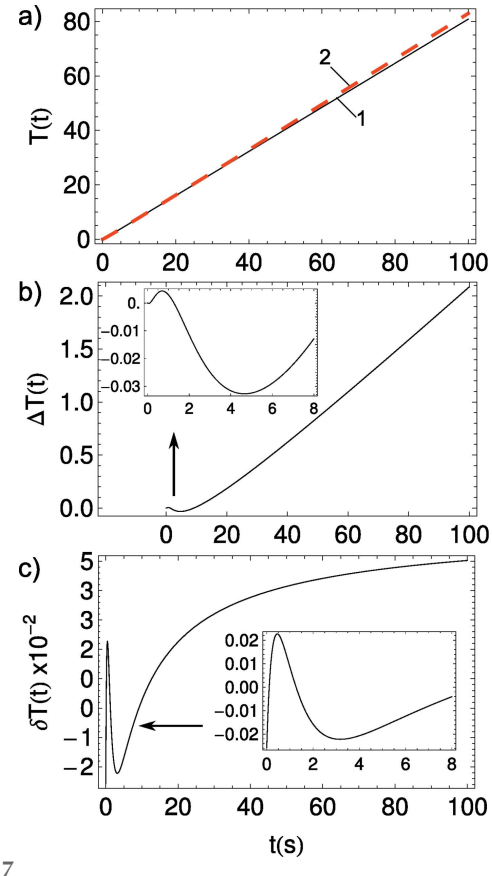

Figure 7
$T(t)$ for two models of $A(t)$. (*a*) The solid black line (1) is for model 1 (exponential), and the red dashed line (2) is for model 2 (hyperbolic). (*b*) Difference between model 2 and model 1 approximations. (*c*) Relative difference of model 1 with respect to model 2, ratio of (*b*) to (*a*) red dashed curve. All inserts have the same axis scaling as the parent panel.

constant sample mass, respectively. This approach can be further extended to $\overline{D}(t) = \overline{E}(t)/\overline{M}(t)$, where the sample mass is no longer assumed to be constant but is treated as an effective function, similar to the dose and absorbed energy. This we call the extended Wang method. In this section we compare the difference between the original Wang method, our extended Wang method and all the methods introduced above in this article. We discuss both $A(t)$ models; however, the formulae are presented for the exponential $A(t)$ (model 1) since the Wang method historically used this model. The PFSA STXM data set [Fig. 3(*a*), blue triangles (2)] is used for the method comparison. First, we derive the formulae for calculating the dose using the original and extended Wang method. Then, we convert them into the form of the $T(t)$ function used above for the dose analysis.

Applying the BL law to the expression for the effective energy absorbed over the time interval $(0,t)$ gives

$$\overline{E}(t) = ei_0\{1 - \exp[-\overline{A}(t)]\}t/k(e), \tag{23}$$

where $\overline{A}(t)$ is an effective optical density linked to the moment t. Wang *et al.* calculate $\overline{A}(t)$ as an average with respect to the exposure time,

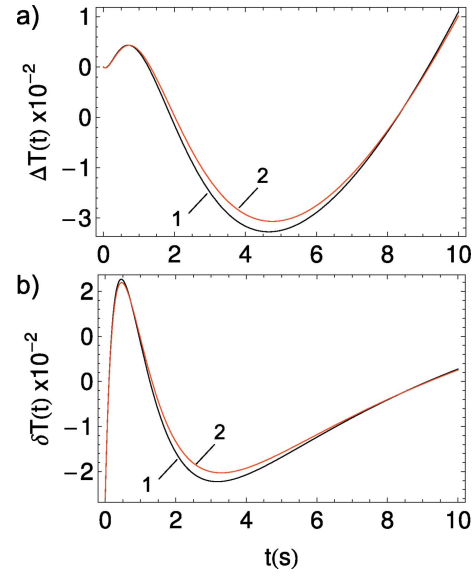

Figure 8
Differences of $T(t)$ estimates. (*a*) Absolute. (*b*) Relative. In (*a*) the black solid curve is the absolute difference of model 2 minus model 1 applied for the exact calculation of $T(t)$; the red solid line is the absolute difference of model 2 minus model 1 applied for the $T(t)$ approximation. Plots in (*b*) correspond to plots presented in (*a*) divided by $T(t)$ calculated for model 2 for the exact and approximated cases, respectively.

$$\overline{A}(t) = t^{-1}\int_0^t A(x)\,\mathrm{d}x, \tag{24}$$

where $A(t)$ is the optical density obtained from STXM data (Figs. 3*a* and 3*b*). This definition coincides with the function $a(t)$ introduced in §3.3. Applying the exponential approximation $A(t) = c + a\exp(-bt)$, the integral can be evaluated from equation (24) analytically to obtain the effective optical density,

$$\overline{A}(t) = c + a\,[1 - \exp(-bt)]/(bt). \tag{25}$$

Similarly, applying the hyperbolic model $A(t) = c + a/(b + t)$, the time average integral $\overline{A}(t)$ equation (24) has the following solution,

$$\overline{A}(t) = c + a\ln(1 + t/b)/t. \tag{26}$$

Fig. 10 presents the effective $\overline{A}(t)$ (dashed curves) and instantaneous $A(t)$ (solid curves) approximations for both models 1 (black) and 2 (red). It is apparent that the effective method overestimates the optical density at all t.

In general, the sample mass is a function of optical density $M(t) = \rho s\,\mu(e)^{-1}A(t)$. Therefore, the original Wang method takes $A(t = 0)$ and calculates the sample mass at $t = 0$, which gives

$$M = \rho s\,\mu(e)^{-1}(c + a), \tag{27}$$

for the exponential $A(t)$ model. Our extended interpretation gives a more general formula for the sample mass,

$$\overline{M}(t) = \rho s\,\mu(e)^{-1}\,\overline{A}(t). \tag{28}$$

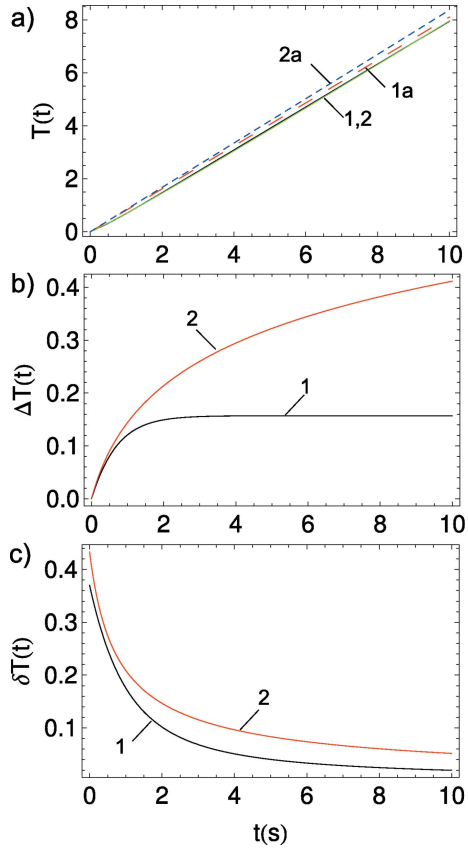

Figure 9
$T(t)$ integral as a function of exposure time using the main term of the asymptotic expression for the two models of $A(t)$. (*a*) Exact integration for $T(t)$: model 1 (1, black solid) and model 2 (2, green solid); the asymptotic solution: model 1 (1a, red large dashed) and model 2 (2a, blue small dashed). (*b*) Absolute $T(t)$ differences of asymptotic and exact solutions for model 1 (black, 1) and model 2 (red, 2), respectively. (*c*) Relative $T(t)$ difference: the difference presented in (*b*) divided by the exact solution for model 1 (black, 1) and model 2 (red, 2), respectively.

Substituting $\overline{E}(t)$ and sample masses, the expressions for the dose become

$$\overline{D}_{\rm o}(t) = \frac{ei_0\,\mu(e)}{k(e)\rho s}\,\frac{1-\exp\left[-\overline{A}(t)\right]}{(c+a)}\,t \qquad (29)$$

for the original Wang method [exponential $A(t)$] and

$$\overline{D}_{\rm e}(t) = \frac{ei_0\,\mu(e)}{k(e)\rho s}\,\frac{1-\exp\left[-\overline{A}(t)\right]}{\overline{A}(t)}\,t \qquad (30)$$

for the extended Wang method. Introducing $R(e)$ we obtain two new $T(t)$ functions,

$$\overline{T}_{\rm o}(t) = \frac{1-\exp\left[-\overline{A}(t)\right]}{(c+a)}\,t \qquad (31)$$

for the original [exponential $A(t)$] Wang method and

$$\overline{T}_{\rm e}(t) = \frac{1-\exp\left[-\overline{A}(t)\right]}{\overline{A}(t)}\,t \qquad (32)$$

for the extended Wang method. Figs. 11 and 12 compare the $T(t)$ functions calculated for both Wang methods with the $T(t)$

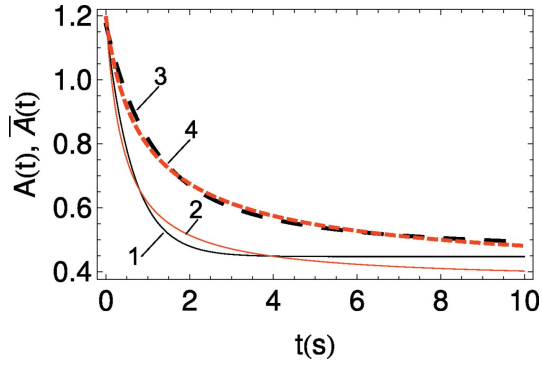

Figure 10
Comparison of instantaneous $A(t)$ and effective $\overline{A}(t)$ (averaged) optical densities calculated for the Wang method. Black (1, 3) is model 1 (exponential) and red (2, 4) is model 2 (hyperbolic). Solid curves (1, 2) are the instantaneous $A(t)$ – an approximation of the direct STXM data; dashed curves (3, 4) are the effective $\overline{A}(t)$ (averaged) over the time interval t.

functions developed for the exact integration, the functional approximation and the asymptotic solutions. Note that it is possible to obtain the formulae for dose and $T(t)$ function for the hyperbolic $A(t)$ model as well. These equations are very similar to those given above except that the equations for $\overline{D}_{\rm o}(t)$, equation (29), and $\overline{T}_{\rm o}(t)$, equation (31), for the hyperbolic $A(t)$ model require the replacement of a by a/b in the denominator. Both hyperbolic and exponential models give similar values for $\overline{T}_{\rm o}(t)$ and $\overline{T}_{\rm e}(t)$ (Fig. 11).

Fig. 11(*a*) shows that the original Wang method underestimates the $T(t)$ function, *i.e.* the dose value compared with our extended version of the Wang method. Fig. 11(*b*) plots the difference between the original and extended Wang methods for various $A(t)$ approximation models. Both $A(t)$ models in Fig. 11(*b*) are in good agreement, indicating that the difference between the original ('o' red curves) and extended ('e' black curves) Wang methods is not due to the $A(t)$ approximation models but to different denominators in the original equation (31) and extended equation (32). The relative difference between the original and extended Wang methods presented in Fig. 11(*c*) reaches ∼60% for long exposure.

Fig. 12(*a*) compares the effective time integral $T(t)$ for all methods, using model 1 (exponential) for optical density $A(t)$ and one selected STXM data set (#2 in Fig. 3). In addition to the equations and methods developed for estimating instantaneous dose, this is one of the key results of this article. Although this figure is presented for model 1 it will be nearly the same for model 2. There are two important messages in Fig. 12(*a*). First, if the changes of the sample mass with radiation damage are taken into account using the extended Wang method, curve (4), the dose can be estimated relatively accurately compared with the exact calculation, curve (1). Second, Fig. 12(*a*) shows that the dose can be treated quite accurately as $D(e,t) \simeq K(e)\,t$ for large times. Therefore, if D is expressed in terms of a rescaled time, the dependence of optical density on the absorbed dose $A(D)$ for large times is similar to $A(t)$.

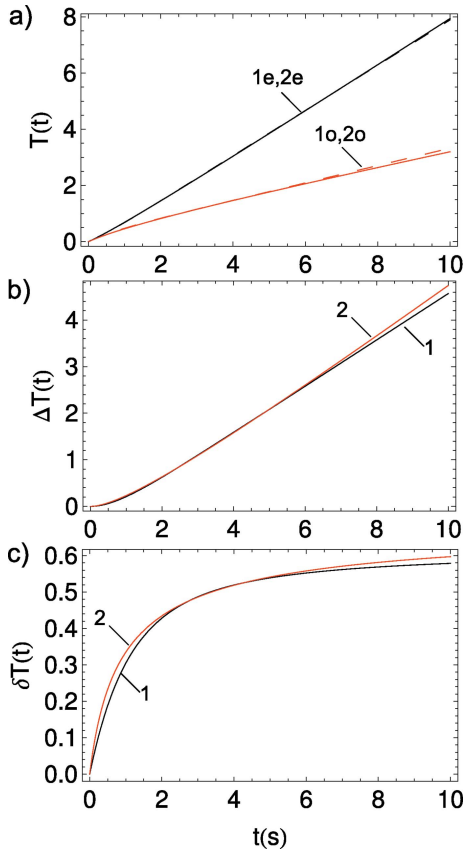

Figure 11
Comparison of $T(t)$ for original (index 'o') and extended (index 'e') Wang methods. (*a*) For two $A(t)$ approximation models: exponential (1, black dashed) and hyperbolic (2, black solid). (*b*) Difference between the extended and original methods. (*c*) Relative difference when (*b*) is divided by the extended $T(t)$ Wang method. In both (*b*) and (*c*) the exponential $A(t)$ model is (1, black) and the hyperbolic $A(t)$ model is (2, red).

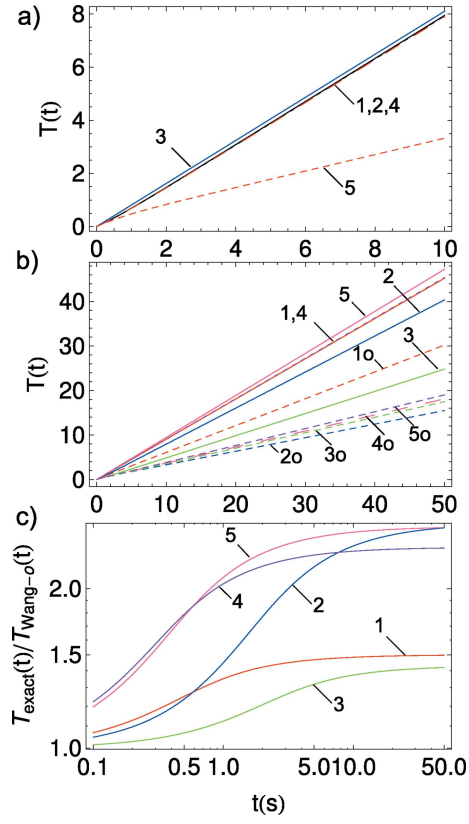

Figure 12
Comparison of the effective time integral $T(t)$ for all methods applied for $A(t)$ model 1 (exponential). (*a*) Exact $T(t)$ integration (1, black solid); $T(t)$ approximation (2, black dashed); asymptote of $T(t)$ (3, blue solid); extended Wang method with non-constant sample mass (4, red solid); original Wang method with constant sample mass (5, red dashed). (*b*) $T(t)$ calculated for all data presented in Fig. 3 applying model 1 for $A(t)$. Curve numbers are the same as the symbol numbers in Fig. 3: single numbers (solid curves) are the exact $T(t)$ calculations whereas the numbers with an index 'o' (dashed curves) are from the original Wang method. (*c*) Ratio of the exact $T(t)$ to the Wang original $T(t)$; the curve indexing follows the rule: red curve, (1) is a ratio of the curves 1 and 1o presented in (*b*), and so on.

Fig. 12(*b*) shows the results of calculating the effective time integral $T(t)$ for all STXM data sets presented in Figs. 3 and 4. Only the exact and the original Wang methods for calculating $T(t)$ were used. Note that having multiple $T(t)$ curves on one plot does not allow their $D(e, t)$ to be compared since they all have different $R(e)$ constants. However, we can compare two methods of $T(t)$ calculation for each data set: the solid line with the dashed line of similar color (curve number, 'o' means original Wang method). The bi-natural logarithm scaled plot, Fig. 12(*c*), shows how much the original Wang method underestimates $T(t)$. For short exposures, where not much material is damaged, the underestimation is relatively small. However, for longer exposures the change of mass due to radiation damage is significant and needs to be taken into account. If the exposure time is large, then both methods reach their own asymptotes and the underestimation ratio becomes constant for all data.

7. Conclusion

We have developed a method for calculating the absorbed dose of X-ray radiation in the case of fixed photon energy (monochromatic beam) and continuous exposure. This is a first rigorous attempt of calculating the absorbed dose for transmitted radiation when the sample undergoes mass loss under X-ray exposure. The derived large time asymptotics and its functional approximations in general form significantly simplify the dose estimation. The exact dose calculation is also performed as an analytical evaluation of the dose integral. In this case the model of optical density evolution with time must be known (measured). Two models of time-dependent optical densities were considered: exponential – related to first-order kinetics; and hyperbolic – related to second-order kinetics of the chemical reactions causing the optical density time decay. The analytical expressions for dose evaluation are presented for both models in order to match a variety of experimental conditions.

The method of dose calculation is tested on the dose experiments conducted with two materials: PFSA (Nafion™) and poly(methylmethacrylate) (PMMA), for which the STXM dose study involving 9-pad measurements was applied. Both

optical density time evolution models, *i.e.* exponential and hyperbolic, were used to calculate the dose for the long time asymptote, exact analytical expression, and its functional approximation (six attempts in total). All six calculations give very similar dose evolution profiles.

These dose calculation methods were compared with the Wang method which ignores mass loss. It was found that the latter significantly underestimates the dose. To fix this problem we developed an extended Wang method and showed that it coincides with our general approximation method and can estimate doses with an accuracy similar to all other methods.

Analysis of available 9-pad STXM data for PFSA and PMMA materials shows that both optical density approximation models can fit the measured $A(t)$ functionalities. Although this does not affect the dose calculation, it does qualitatively affect the assumption of the particular kinetics of X-ray damage. This is quite important and was not noticed or discussed before. We stress that currently the evidence for a specific type of kinetics is mostly heuristic rather than rigorous. Indeed, if the experimental data can fit model 1, then the reaction kinetics behind the observed $A(t)$ decay is assumed to be of first order. Ambiguity appears when the same $A(t)$ data can fit another function – the hyperbolic decay $A(t) = c + a/(b + t)$ model 2, corresponding to second-order reaction kinetics. If both models can fit the same $A(t)$ data with similar accuracy then one must conclude that the given $A(t)$ shape is not sensitive to the kinetic order and other independent considerations are required to resolve this issue. It appears that the presented accuracy of 9-pad STXM data cannot support a claim on the order of kinetics of the photochemical reactions happening during X-ray irradiation. Such a claim requires either an increase of STXM accuracy or some other independent methods from which the kinetic order can be determined with more accuracy. Why the absorbed dose is affected very little by the order of kinetics is unclear and must be understood in the light of photo-chemistry.

It is worth mentioning possible generalizations of the presented dose calculation. The optical density in general is a function of two variables $A(e, t)$. In the current manuscript only the time-dependent part $A(t)$ for the fixed e was considered corresponding to continuous absorption of *monochromatic* X-rays. This is the case of STXM experiments (and other experiments which use a monochromatic X-ray beam) for which the sample mass loss due to X-ray irradiation is documented, measured and analysed. The case where time t is fixed and the applied X-ray beam is *continuously distributed* in the photon energy interval (e_1, e_2) corresponds to a quite different set of experiments. The first-principles approach presented here allows extension of these results to a more general expression for dose calculation, including integration over the photon energy interval.

Another possible generalization takes into account chemical changes in the sample materials due to breaking the existing bonds or establishing new chemical bonds. To accommodate this type of optical density change we need to allow μ (the standard absorption coefficient) to be a function of time, $\mu(t)$. In this case the above approach requires another extension. The current definition of μ is valid for any elapsed time t when μ does not change significantly: $\mu(t_0 + \delta t) = \mu_0 + \mu'(t)\,\delta t$, where we neglect the linear term. At the same time, we allow for significant changes in optical density attributing it to mass loss. Data for $\mu(t)$ evolution as a function of dose are available. Extension of this methodology to treat those cases will be of interest and is being explored.

APPENDIX *A*
Derivation of BL dose integral

The rate of the absorbed photons $[i_0 - i(t)]/k$ multiplied by the photon energy e gives the rate of energy absorption $\dot{E}(e, t) = e[i_0 - i(t)]/k$. Taking into account the BL model $i(t) = i_0 \exp[-A(t)]$ the rate of energy absorption is $\dot{E}(e, t) = e\{i_0 - i_0 \exp[-A(t)]\}/k = ei_0\{1 - \exp[-A(t)]\}/k$.

The mass $M(t)$ of the material is a product of the cross-sectional area of the beam s, the material density ρ and the sample thickness $h(t)$: $M(t) = h(t)\rho s$. The thickness of the sample can be expressed in terms of the optical density $A(t)$ and the standard absorption coefficient μ, $h(t) = A(t)/\mu$. Thus, an expression for the mass reads $M(t) = A(t)\rho s/\mu$.

Substituting $\dot{E}(e, t)$ and $M(t)$ in the integral of equation (2) we have

$$D(e, t) = \int_0^t \frac{ei_0\,\mu}{k\rho s}\,\frac{1 - \exp[-A(x)]}{A(x)}\,\mathrm{d}x. \tag{33}$$

Here i_0, μ and k are the functions of the photon energy e independent of time and therefore they can be moved from the integral leading to equation (3),

$$D(e, t) = \frac{ei_0\,\mu(e)}{k(e)\,\rho s}\int_0^t \frac{1 - \exp[-A(x)]}{A(x)}\,\mathrm{d}x. \tag{34}$$

APPENDIX *B*
Asymptotics of the dose integral

The interval of the $A(t)$ argument can be split into two segments: $0 < t < t^*$ where $A(t)$ changes significantly, and $t > t^*$ where $A(t) \simeq A_\infty$. The dose is also split into two terms, $D(e, t) = R(e)\,T(t)$, where $T(t) = T(t^*) + T(t > t^*)$, with respect to the time segments. Using $T(t)$ from equation (4) in both terms, and substituting $A(t) \simeq A_\infty$ in the second term, we have, respectively,

$$\begin{aligned} T(t^*) &= \int_0^{t^*} \frac{1 - \exp[-A(x)]}{A(x)}\,\mathrm{d}x, \\ T(t > t^*) &= \int_{t^*}^{t} \frac{1 - \exp(-A_\infty)}{A_\infty}\,\mathrm{d}x \;=\; B(t - t^*), \end{aligned} \tag{35}$$

where we introduce a constant $B = [1 - \exp(-A_\infty)]/A_\infty$. The integral of the first term can be evaluated either *via* the

analytical integration or the approximation; the result of both cases produces some constant $C(t^*)$ depending on t^*.

APPENDIX C
Approximation of the dose integral

First we show that, for a typical behavior of optical density $A(t)$ (monotonic change and approach to some asymptotic constant value) for the approximation suggested in §3.3, the residual does not grow with exposure time. Note that in the asymptotic range where changes in $A(t)$ can be neglected, $A(t) = a(t) + a'(t)\,t = \text{const}$, which is possible only when $a'(t) = 0$ and $a(t) = \text{const}$ with $a'(t)\,t$ approaching zero. Expanding equation (11) by adding a residual term $O(t)$ which we are going to estimate gives

$$T(t) = \int_0^t \left\{\frac{1-\exp[-A(x)]}{A(x)}\right\} \mathrm{d}x = \frac{1-\exp[-a(t)]}{a(t)}\,t + O(t) = T_a(t) + O(t). \quad (36)$$

Finding the derivative of the residue $O'(t) = (\{1-\exp[-A(t)]\}/A(t)) - T_a'(t)$, substituting $A(t) = a(t) + a'(t)\,t$ into the first term and expanding in a series in $a'(t)$, retaining the first non-vanishing order gives

$$O'(t) \simeq H[a(t)][ta'(t)]^2, \quad (37)$$

where

$$H(x) = \left[1 - \left(1 + x + x^2/2\right)\exp(-x)\right]/x^3, \quad (38)$$

where $H(x)$ is a positive, finite and decreasing function. Thus at large exposure times the residue derivative tends to zero, so that the residue itself does not grow.

The value of the residue at large times is then estimated. Similarly to the asymptotic analysis performed in Appendix B, we split the time interval into two parts, $0 < t < t^*$ and $t > t^*$, and consider the computation in each segment. Thus we have $T_a(t) = T_a(t^*) + T_a(t > t^*)$, where the choice of t^* is defined by the condition $|A(t^*) - A(t)| = \varepsilon$, where $\varepsilon \ll 1$ is a small parameter, and $t^*(\varepsilon)$ depends on this small parameter. Thus we obtain

$$T_a(t^*) \simeq \frac{1-\exp[-a(t^*)]}{a(t^*)}\,t^*$$

and

$$T_a(t > t^*) \simeq \frac{1-\exp(-A^*)}{A^*}(t - t^*),$$

where we denote $A(t^*) = A^*$. For $t > t^*$ the difference between the values A^* and A_∞ is of the order of small ε and can be neglected, so that $T(t > t^*) = T_a(t > t^*)$. Thus we find that the residue $O(t) = T(t) - T_a(t) = T(t^*) - T_a(t^*) = O(t^*)$ is determined solely by the initial time interval $0 < t < t^*$. This value is computed explicitly to obtain

$$O(t^*) = T(t^*) - T_a(t^*) = \int_0^{t^*} \frac{1-\exp[-A(x)]}{A(x)}\,\mathrm{d}x - \frac{1-\exp[-a(t^*)]}{a(t^*)}\,t^*. \quad (39)$$

Note that the residual of our approximation $tF[a(t)]$ is defined by the interval $0 < t < t^*$ only; thus $O(t)$ is a constant and its value depends on t^* and the particular functionality of the optical density $A(t)$, which is found from fitting STXM data like those presented in Fig. 1. Having an approximation for $A(t)$, we can find $a(t^*)$ explicitly and then estimate the value of the residual numerically.

APPENDIX D
Full expressions for exactly integrated $T(t)$

D1. Model 1

$$T(t) = \frac{-\exp(-c)\,Ei(-a) + Ei(-c-a) + \ln(a) - \ln(c+a)}{bc} + \frac{\exp(-c)\,Ei(c-y) - Ei(-y) + \ln(y) - \ln(-c+y)}{bc}, \quad (40)$$

where $y = c + a\exp(-bt)$ must be substituted.

D2. Model 2

$$T(t) = -\frac{b[1-\exp(-a/b-c)]}{c} - \frac{a[1-\exp(-y)]}{c(c-y)} + \frac{a}{c^2}\left[\exp(-c)\,Ei\left(-\frac{a}{b}\right) + c\exp(-c)\,Ei\left(-\frac{a}{b}\right) - Ei\left(-\frac{a}{b}-c\right) - \ln\left(-\frac{a}{b}\right) + \ln\left(-\frac{a}{b}-c\right)\right] - \frac{a}{c^2}\left[\exp(-c)\,Ei(c-y) + c\exp(-c)\,Ei(c-y) - Ei(-y) - \ln(c-y) + \ln(-y)\right], \quad (41)$$

where $y = c + a/(b+t)$ must be substituted.

Acknowledgements

Research supported by the Natural Sciences and Engineering Research Council (NSERC) Discovery grant and the CaRPE-FC network. STXM measurements were performed using STXMs on beamlines 5.3.2.2 and 11.0.2 at the Advanced Light Source (ALS) which is supported by the Division of Basic Energy Sciences of the US Department of Energy under contract No. DE-AC02-05CH11231. Measurements were also made using the ambient STXM on beamline 10ID1 at the Canadian Light Source (CLS), which is supported by CFI, NSERC, CIHR, NRC and the University of Saskatchewan. We thank staff scientists, David Kilcoyne and Tolek Tyliszczak at ALS and Jian Wang at CLS for their assistance and support of the beamline and STXMs. We thank Adam Leontowich for

providing 9-pad dose-damage data for PMMA used in this work.

Funding information

The following funding is acknowledged: Natural Sciences and Engineering Research Council Discovery grant; CaRPE-FC network; Division of Basic Energy Sciences of the US Department of Energy (contract No. DE-AC02-05CH11231).

References

Ade, H. & Hitchcock, A. P. (2008). *Polymer*, **49**, 643–675.
Aglincev, K. K. (1957). *Dosimetry of Ionizing Radiation*, 2nd ed. (In Russian.) Moscow: Gos. Izd. Tech-Teor Lit.
Attix, F. H. (1986). *Introduction to Radiological Physics and Radiation Dosimetry*. New York: John Wiley and Sons.
Beetz, T. & Jacobsen, C. (2003). *J. Synchrotron Rad.* **10**, 280–283.
Berejnov, V., Susac, D., Stumper, J. & Hitchcock, A. P. (2013). *ECS Trans.* **50**, 361–368.
Borek, D., Cymborowski, M., Machius, M., Minor, W. & Otwinowski, Z. (2010). *Acta Cryst.* D**66**, 426–436.
Coffey, T., Urquhart, S. G. & Ade, H. (2002). *J. Electron Spectrosc. Relat. Phenom.* **122**, 65–78.
Collins, B. A. & Ade, H. (2012). *J. Electron Spectrosc. Relat. Phenom.* **185**, 119–128.
Henke, B. L., Gullikson, E. M. & Davis, J. C. (1993). *At. Data Nucl. Data Tables*, **54**, 181–342.
Hitchcock, A. P., Obst, M., Wang, J., Lu, Y. S. & Tyliszczak, T. (2012). *Environ. Sci. Technol.* **46**, 2821–2829.
Hitchcock, A. P., Wang, J., Botton, G. A. & Egerton, R. F. (2005). *Microsc. Microanal.* **11**, 2046–2047.
Howells, M. R., Hitchcock, A. P. & Jacobsen, C. J. (2009). *J. Electron Spectrosc. Relat. Phenom.* **170**, 1–3.
Jacobsen, C., Wirick, S., Flynn, G. & Zimba, C. (2000). *J. Microsc.* **197**, 173–184.
Kase, K. R. & Nelson, W. R. (1978). *Concepts of Radiation Dosimetry*. New York: Pergamon Press.
Kaznatcheev, K. V., Karunakaran, C., Lanke, U. D., Urquhart, S. G., Obst, M. & Hitchcock, A. P. (2007). *Nucl. Instrum. Methods Phys. Res. A*, **582**, 96–99.
Kilcoyne, A. L. D., Tyliszczak, T., Steele, W. F., Fakra, S., Hitchcock, P., Franck, K., Anderson, E., Harteneck, B., Rightor, E. G., Mitchell, G. E., Hitchcock, A. P., Yang, L., Warwick, T. & Ade, H. (2003). *J. Synchrotron Rad.* **10**, 125–136.
Kmetko, J., Husseini, N. S., Naides, M., Kalinin, Y. & Thorne, R. E. (2006). *Acta Cryst.* D**62**, 1030–1038.
Leontowich, A. F. G. (2012). PhD thesis, McMaster University, Canada.
Leontowich, A. F. G. (2013). *Radiat. Phys. Chem.* **90**, 87–91.
Leontowich, A. F. G. & Hitchcock, A. P. (2011). *Appl. Phys. A*, **103**, 1–11.
Leontowich, A. F. G., Hitchcock, A. P. & Egerton, R. F. (2016). *J. Electron Spectrosc. Relat. Phenom.* **206**, 58–64.
Leontowich, A. F. G., Hitchcock, A. P., Tyliszczak, T., Weigand, M., Wang, J. & Karunakaran, C. (2012). *J. Synchrotron Rad.* **19**, 976–987.
Leontowich, A. F. G., Hitchcock, A. P., Watts, B. & Raabe, J. (2013). *Microelectron. Eng.* **108**, 5–7.
Leontowich, A. F. G., Tyliszczak, T. & Hitchcock, A. P. (2011). *Proc. SPIE*, **8077**, 80770N.
Paithankar, K. S. & Garman, E. F. (2010). *Acta Cryst.* D**66**, 381–388.
Pikaev, A. K. (1975). *Dosimetry for Radiaiton Chemistry*. (In Russian.) Moscow: Nauka.
Schooneveld, M. M. van & DeBeer, S. (2015). *J. Electron Spectrosc. Relat. Phenom.* **198**, 31–56.
Schuettfort, T., Watts, B., Thomsen, L., Lee, M., Sirringhaus, H. & McNeill, C. R. (2012). *ACS Nano*, **6**, 1849–1864.
Seltzer, S. M., Bartlett, D. T., Burns, D. T., Dietze, G., Menzel, H.-G., Paretzke, H. G. & Wambersie, A. (2011). *J. ICRU*, **11**, 1–31.
Sliz, P., Harrison, S. C. & Rosenbaum, G. (2003). *Structure*, **11**, 13–19.
Stöhr, J. (1992). *NEXAFS Spectroscopy*, 2nd ed. New York: Springer.
Stolz, W. & Bernhardt, R. (1981). *Dosimetrie Ionisierender Strahlung*. (In German.) Berlin: Akademie-Verlag.
Susac, D., Berejnov, V., Hitchcock, A. P. & Stumper, J. (2011). *ECS Trans.*, **41**, 629–635.
Tzvetkov, G., Späth, A. & Fink, R. H. (2014). *Radiat. Phys. Chem.* **103**, 84–88.
Urquhart, S. G., Hitchcock, A. P., Smith, A. P., Ade, H. W., Lidy, W., Rightor, E. G. & Mitchell, G. E. (1999). *J. Electron Spectrosc. Relat. Phenom.* **100**, 119–135.
Wang, J. (2008). PhD thesis, McMaster University, Canada.
Wang, J., Botton, G. A., West, M. M. & Hitchcock, A. P. (2009). *J. Phys. Chem. B*, **113**, 1869–1876.
Wang, J., Morin, C., Li, L., Hitchcock, A. P., Scholl, A. & Doran, A. (2009). *J. Electron Spectrosc. Relat. Phenom.* **170**, 25–36.
Wang, J., Stöver, H. D. H. & Hitchcock, A. P. (2007). *J. Phys. Chem. C*, **111**, 16330–16338.
Wang, J., Stöver, H. D. H., Hitchcock, A. P. & Tyliszczak, T. (2007). *J. Synchrotron Rad.* **14**, 181–190.
Watts, B., McNeill, C. R. & Raabe, J. (2012). *Synth. Met.* **161**, 2516–2520.
Zhang, X., Jacobsen, C., Lindaas, S. & Williams, S. (1995). *J. Vac. Sci. Technol. B*, **13**, 1477–1483.